

CHAPTER II

THEORY AND LITERATURE REVIEW

2.1 Natural Rubber

Natural rubber can be obtained from nearly 2000 different plant species yield polymer akin to natural rubber and that rubber of sorts have been obtained from some 500 of them. To all intents and purposes, the natural rubber of commerce is obtained from the latex of *Hevea brasiliensis*, a native of Brazil but widely grown on plantations in tropical Africa and Asia. The production of natural rubber has grown steadily since World War II. The Southeast Asian region accounted for about 80% of the total production. The conversion of natural rubber into products is accomplished in many different ways [1].

2.1.1 The Chemical Formula of Natural Rubber

The empirical formula for the natural rubber (NR) molecule appears to have been first determined by Faraday who reported his finding in 1826. He concluded that carbon and hydrogen were the only elements present and his results correspond to the formula C_5H_8 . This result was obtained using a product which contains associated non-rubber material. Subsequent studies with highly purified materials have confirmed Faraday's conclusion [1]. Isoprene was found to have the formula C_5H_8 , for which Tilden proposed the structure.

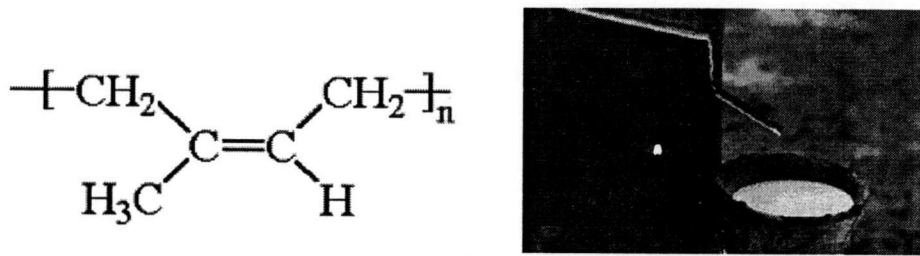


Figure 2.1 Isoprene unit and fresh natural rubber latex [2]

The linear structure proposed by Pickles provided the possibility of structural isomer with both *cis*- and *trans*- repeating units. In fact, the natural rubber molecule is not a pure *cis*-1, 4 polyisoprene. Besides, it contains very small amounts of functional groups in rubber chain termed as abnormal groups, such as aldehyde groups [3], ester or lactone group [4], and epoxides [5,6]. Structural studies using ^{13}C -NMR spectroscopy disclosed that the rubber molecule contains about two to three *trans* isoprene units [7]. Recently, detailed structure characterization of natural rubber was investigated by ^{13}C -NMR and ^1H -NMR spectroscopies [8, 9]. From the relative intensity of the signal and the degree of polymerization of highly purified natural rubber, the number of *trans* isoprene existing at the initiating terminal of the rubber molecule is estimated to be two. Accordingly, the structure of natural rubber is assumed to be as shown in Figure 2.2.

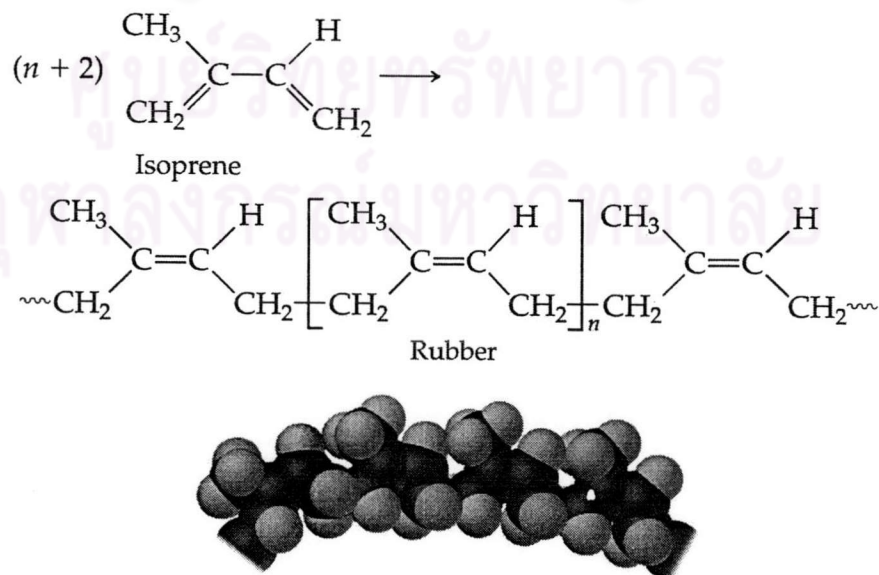


Figure 2.2 Presumed structure of natural rubber [10].

2.1.2 Composition of Natural Rubber

The chemical composition of fresh *Hevea* latex is complex when compared to synthetic latex. This is because fresh *Hevea* latex is a cycloplasm. It has been known for a long time that fresh *Hevea* latex contains, in addition to rubber hydrocarbon, a large number of non-rubber constituents (many proteinous and resinous substances, carbohydrates, inorganic matter, water, *etc.*) present in relatively small amounts. Many of these are dissolved in the aqueous serum of the latex, others are adsorbed at the surface of the rubber particles and the non-rubber particles suspended in latex [3]. The typical composition of natural rubber and fresh latex is shown in Table 2.1.

Table 2.1 Typical composition of fresh *Hevea* latex [11].

Ingredient	Average value (%w/w)
Total solid content	36.0
Dry rubber	33.0
Proteinous substance	1.0-1.5
Resinous substance	1.0-2.5
Carbohydrate	1.0
Inorganic matter	Up to 1.0

2.1.3 Physical Properties [10]

Physical properties of natural rubber may slightly be due to the non-rubber constituents present and to degree of crystallinity. When the natural rubber is held below 10°C, crystallization occurs, resulting in the change of density from 0.92 to about 0.95. The average molecular weight can range from 200,000-500,000. Some average physical properties of natural rubber are shown in Table 2.2.

Table 2.2 Some physical properties of natural rubber. [11]

Properties	Value
Density	0.92
Refractive index (20°C)	1.52
Coefficient of cubical expansion	0.00062/°C
Cohesive energy density	63.7 cal./c.c.
Heat of combustion	10,700 cal/g.
Thermal conductivity	0.00032 cal./sec./cm ² /°C
Dielectric constant	2.37
Power factor (1,000 cycles)	0.15-0.2
Volume resistivity	10 ¹⁵ ohms/c.c.
Dielectric strength	1,000 volts/mm ²

2.2 Vulcanization [12]

Useful rubber articles, such as tired and mechanical goods, cannot be made without vulcanization. Unvulcanized rubber is generally not very strong, does not maintain its shape after large deformation and can be very sticky. Vulcanization can be defined as a process which increase the retractile force and reduces the amount of permanent deformation remaining after removal of the deformation force. Thus, vulcanization increases elasticity while it decreases plasticity. It is generally accomplished by the formation of a crosslinked molecular network.

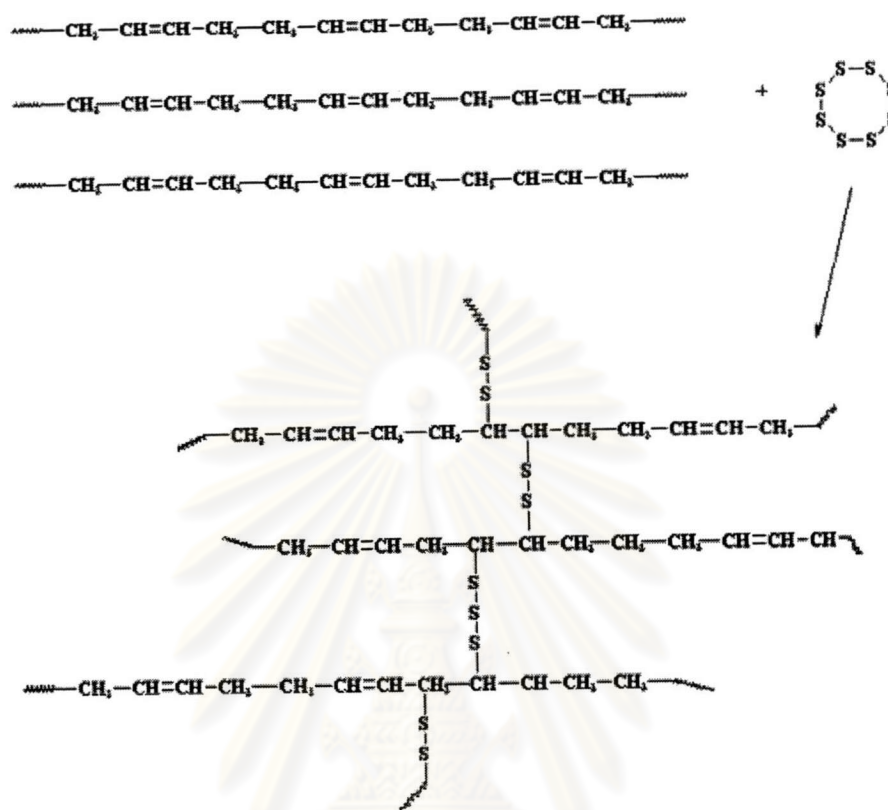


Figure 2.3 Sulfur vulcanized rubber [13].

According to the theory of rubber elasticity, the retractile force to resist a deformation is proportional to the number of network-supporting polymer chain per unit volume of elastomer. A supporting polymer chain is a linear polymer molecule junctures. An increase in the number of junctures or crosslinks gives an increase in the number of supporting chains. In an unvulcanized linear high polymer (above its melting point) only molecular chain entanglements constitute junctures.

Vulcanization is a process of chemically producing network junctures by the insertion of crosslinks between polymer chains. The crosslink may be a group of sulfur atom in a short chain, a single sulfur atom, carbon-to-carbon bond, a polyvalent organic radical, an inorganic cluster, or a polyvalent metal ion. The process is usually carried out by heating the rubber (mixed with vulcanizing agents) in a mold under pressure.

Accelerated-sulfur vulcanization is the most widely used method. For many applications, it is the only rapid crosslinking technique which can, in a practical manner, give the delayed action required for processing, shaping and forming before formation of the intractable vulcanized network. It is used to vulcanize natural rubber, synthetic isoprene rubber, styrene-butadiene rubber, nitrile rubber, butyl rubber, chlorobutyl rubber, bromobutyl rubber and ethylene-propylene-diene monomer rubber.

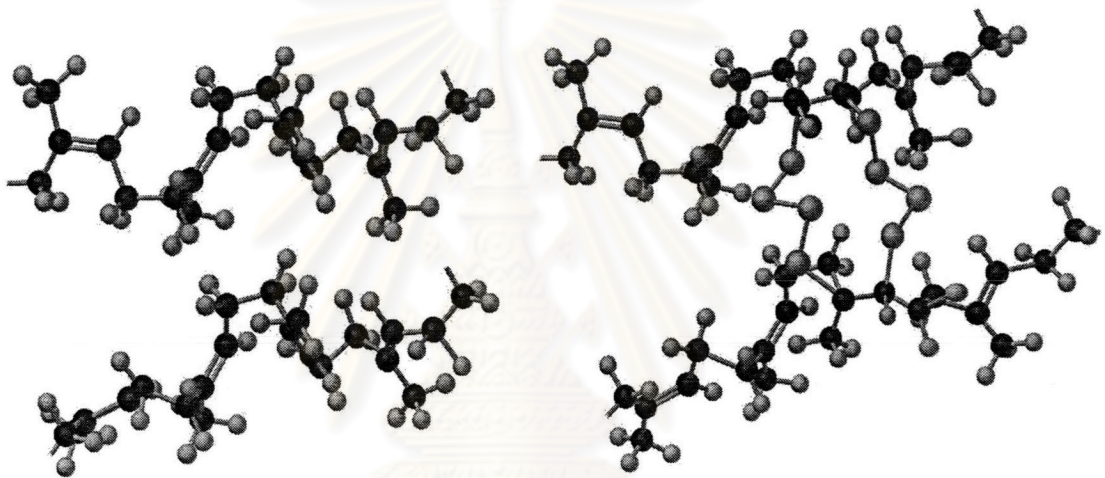
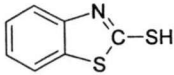
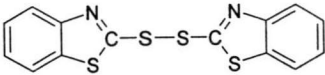
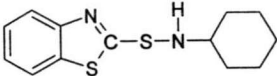
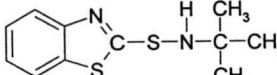
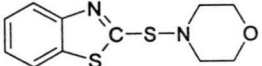
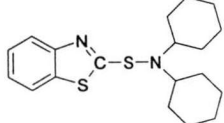
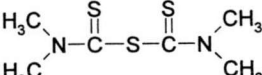
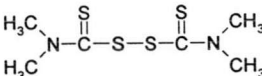
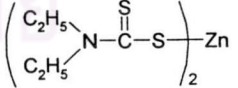
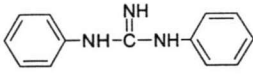
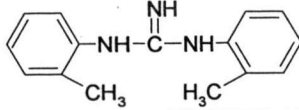


Figure 2.4 Demonstration of sulfur vulcanized rubber molecule [10].

Typically a recipe for the vulcanized system for one of the above elastomer contains 2-10 phr of zinc oxide, 1-4 phr of fatty acid (e.g. stearic acid), 0.5-4 phr of sulfur, and 0.5-2 phr of accelerator. The fatty acid with zinc oxide forms a salt which can form complexes with accelerators and reaction products formed between accelerators and sulfur. Accelerators are classified and illustrated in Table 2.3

Frequently, mixtures of accelerators are used. Typically, a benzothiazole type is used with smaller amounts of a dithiocarbamate (thiuram) or an amine type. An effect of using a mixture of two different types of accelerator can be obtained. Mixing accelerators of the same type gives intermediate or average results.

Table 2.3 Accelerators for sulfur vulcanization [12].

Compound	Abbreviation	Structure
<i>Benzothiazoles</i>		
2-Mercaptobenzothiazole	MBT	
2,2'-Dithiobisbenzothiazole	MBTS	
<i>Benzothiazolesulfenamides</i>		
<i>N</i> -Cyclohexylbenzothiazole-2-sulfenamide	CBS	
<i>N</i> -t-Butylbenzothiazole-2-sulfenamide	TBBS	
2-Morpholinothiobenzothiazole	MBS	
<i>N</i> -Dicyclobenzothiazole-2-sulfenamide	DCBS	
<i>Dithiocarbamates</i>		
Tetramethylthiuram monosulfide	TMTM	
Tetramethylthiuram disulfide	TMTD	
Zinc diethyldithiocarbamate	ZDEC	
<i>Amines</i>		
Diphenylguanidine	DPG	
Di- <i>o</i> -tolylguanidine	DOTG	

2.3 Tests for Mechanical Properties [12]

The stress-strain test in tension, including ultimate tensile and elongation, is probably still the most widely used test in the rubber industry. Among the purposes for such tests are: to ensure that all compounding ingredients have been added in proper proportions, to determine rate of cure and optimum cure for experimental polymers and compounds, for specification purposes and to obtain an over-all quality check on the compounds. Proportionately fewer tensile tests are run now than a previous year, for two principal reasons: the cure meter have been given a large share of the tests for state of cure, and more emphasis is being given to testing for the properties desired in a particular stock than to tests for general quality. High tensile strength is seldom required in service and by itself, does not guarantee the level of any other property. However, since a single test can yield modulus at specified elongation, ultimate elongation, and ultimate tensile strength in well standardized tests and with short testing time, tensile tests are far from outdated. As shown in Figure 2.5 stress is the force per unit cross sectional area (F/A for either tensile or tear deformation). Strain is the deformation per unit original length ($\Delta L/L$) in tensile tests or deformation per unit distance between the contacting surfaces in shear tests.

Stress is usually expressed in unit of newton per square meter (N/m^2). Strain is usually expressed in percent. Since it is the ratio of two lengths, it is dimensionless. An elongation of 300 %, for example, means that the specimen has been stretched to four times its original length.

จุฬาลงกรณ์มหาวิทยาลัย

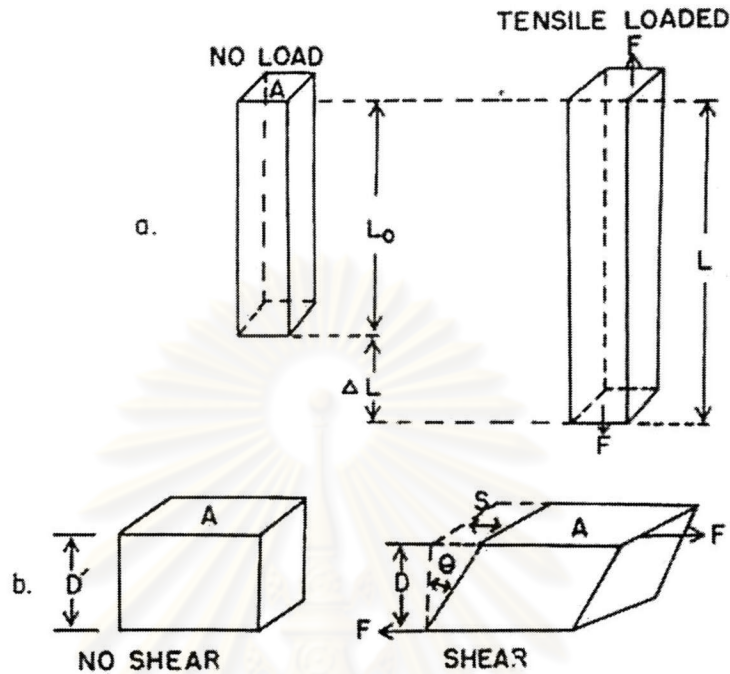


Figure 2.5 Tensile stretching of bar (a), shear of a rectangular block (b) [12].

In the common manner of rubber technology the stress required for a given elongation is used to present the material stiffness. This quantity is called the modulus. A 300 % modulus, for example, means the stress required to produce a 300 % elongation. In mechanical usage, however, the term modulus is said to obey Hooke's law and the constant is called Young's modulus. In practice, the term of modulus is often used to present the ratio of stress to strain even in situations where it may carry with the change in elongation. In the terms used in 2.5 a. Young's modulus (E) is given by:

$$E = (F/A) / \Delta L/L \dots\dots\dots (1)$$

Tensile stress is calculated as a ratio of observed force to the cross-sectional area of the outstretched specimen. Elongation for straight and dumbbell specimens is given by

$$\text{Elongation, percent} = (L-L_0 / L_0) \times 100 \dots\dots\dots (2)$$

2.4 Graft Copolymerization [14-16]

The idea of graft or block copolymerization probably first arose as means of modification naturally occurring polymers, such as cellulose (cotton), rubber, or wool. Graft copolymerization, by analogy to the botanical term, refers to the growth of a branch of different chemical composition on the backbone of the linear macromolecule. The important of this type of polymer structures is due basically to the fact that polymer chains of different chemical structure, which are normally incompatible and form separate phase, are chemically bonded to each other.

Graft copolymerization by free radical reactions has been the most widely applied system for the formation of graft copolymers, as it provides the simplest method and can be used with the wide variety of polymers and monomers. It has not been very useful in the synthesis of block copolymers, as will become obvious from an examination of the method used.

Photopolymerization

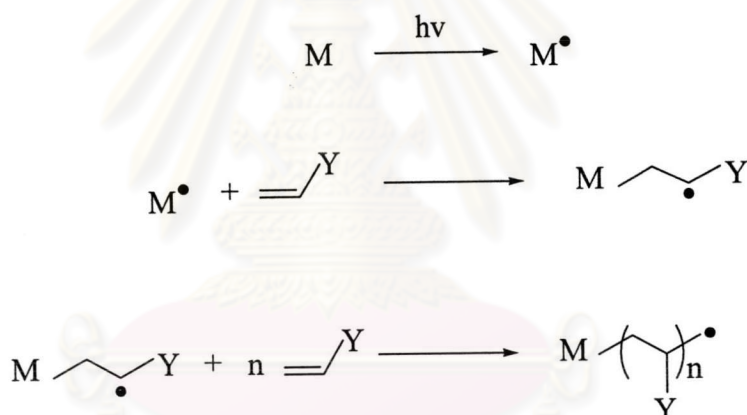
Irradiation has been most widely used to provide active sites for graft copolymerization. This is done with ultraviolet or visible radiation, with or without added photosensitizer, or with ionizing radiation, particularly the latter. Free radical reactions are involved in all cases.

Photochemical or photo initiations occur when radicals are produced by ultraviolet and visible light irradiation of a reaction system. In general, light absorption results in radical production by either of two pathways:

1. Some compound in the system undergoes excitation by energy absorption and subsequent decomposition into radicals.
2. Some compound undergoes excitation and excited species interacts with a second compound (by either energy transfer or redox reaction) to form radicals derived from the latter and/ or formed compound(s).

Table 2.4 Purposes of ultraviolet light [17].

Types of ultraviolet light	Purpose
UVA (315-400 nm)	Backlight. Used for low energy UV polymerization reactions, also for fluorescent inspection purposes.
UVB (280-315 nm)	Used with UVA for polymerization and accelerated light aging materials. Is the light responsible for sun tanning.
UVC (200-280 nm)	Used for rapid surface cure of UV inks and lacquers, also for sterilization and germicidal applications.
VUV (100-200 nm)	Vacuum UV. Can only be used in a vacuum and therefore is of minor commercial importance.

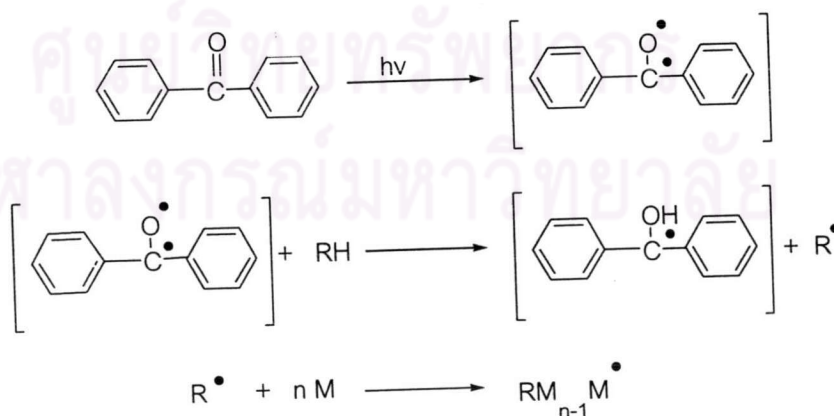
**Scheme 2.1** Photopolymerization process [14].

Most of the polymers cannot absorb light energy directly by themselves. In order for a photopolymerization process to react to UV light, a chemical called a *photoinitiator* must be present in the reaction. Light emitted from a suitable source causes the photoinitiator to fragment into reactive species that are able to convert the absorbed light energy into another useful form and initiate a rapid polymerization process with monomers and oligomers in the systems to form a crosslinked, durable polymer. That's why the photopolymerization reaction essentially consists of the light sensitive compound.

Photosensitizer is an additive present to facilitate the initiation step. It may absorb and then transfer energy to another molecule that forms a primary reactive species, usually free radicals. And may be defined that photosensitizer is the compound that having a positive influence on the photopolymerization reaction rate, may therefore be regarded as a photo-catalyst. Efficient photosensitizer depends upon, giving an appropriate light source, several factors, including

1. Suitable absorption coefficients and wavelength sensitive for the initiators molecule.
2. Important initiation quantum yields in the range 0.1-1.0.
3. The initiator molecule or any of its photo-fragments should not function as chain transfer agents or terminating agents.

There are many kinds of photosensitizer used in photopolymerization reaction such as dimethoxy-2-phenyl acetophenone, 1-phenyl-1, 2-propanedione-2-(O-ethoxycarbonyl oxime), dialkoxyacetophenones. And the most widely used and well known photosensitizer for the UV-induced polymerization reaction is benzophenone and its derivatives. Benzophenone reacts by hydrogen abstraction and is photo-reduced to benzopinacol in the presence of hydrogen donors.



Scheme 2.2 Benzophenone dissociation by UV light [18].

Benzophenone undergoes a photo-induced excitation predominantly at 340 nm to form a singlet excited state which is an isomer of the ground state [19].

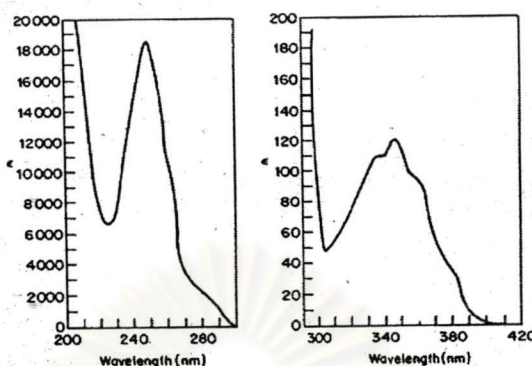


Figure 2.6 Absorption spectra for benzophenone in cyclohexane at 25°C [19].

2.5 Blood Compatibility

Blood compatibility is determined by interactions at the blood-material interface that depend on the material surface chemical structure. It involves complement activation, platelet adhesion and stimulation of plasma coagulation. Endothelial cells produce some substances with antithrombotic action. However, two important aspects of biomaterial screening refer to their *in vitro* cytotoxicity and blood compatibility behavior. Artificial surfaces in contact with blood trigger a number of biological systems through the adsorption of protein and cells. It is generally believed that the nature of adsorbed protein layer determines all adverse events that impair the use of artificial materials in medical devices: thrombus formation as a result of platelet adhesion, platelet activation, initiation of coagulation and activation of the complement system that in turn results in leukocyte adhesion and activation [20, 21].

2.5.1 Human Plasma

Human blood is a highly complex substance. Its major components are red blood cells, which carry oxygen from the lungs to the body; white blood cells, which have major roles in disease prevention and immunity; and platelets, which are key

elements in the blood clotting process. These blood elements are suspended in blood plasma, a yellowish liquid that comprises about 55% of human blood. When the blood was spin in a centrifuge, the red cells go to the bottom of the container, and the white cells and platelets to the middle, leaving the yellowish plasma at the top.

The plasma is the river in which the blood cells travel. It carries not only the blood cells but also nutrients (sugars, amino acids, fats, salts, minerals, etc.), waste products (CO₂, lactic acid, urea, etc.), antibodies, clotting proteins (called clotting factors), chemical messengers such as hormones, and proteins that help maintain the body's fluid balance.

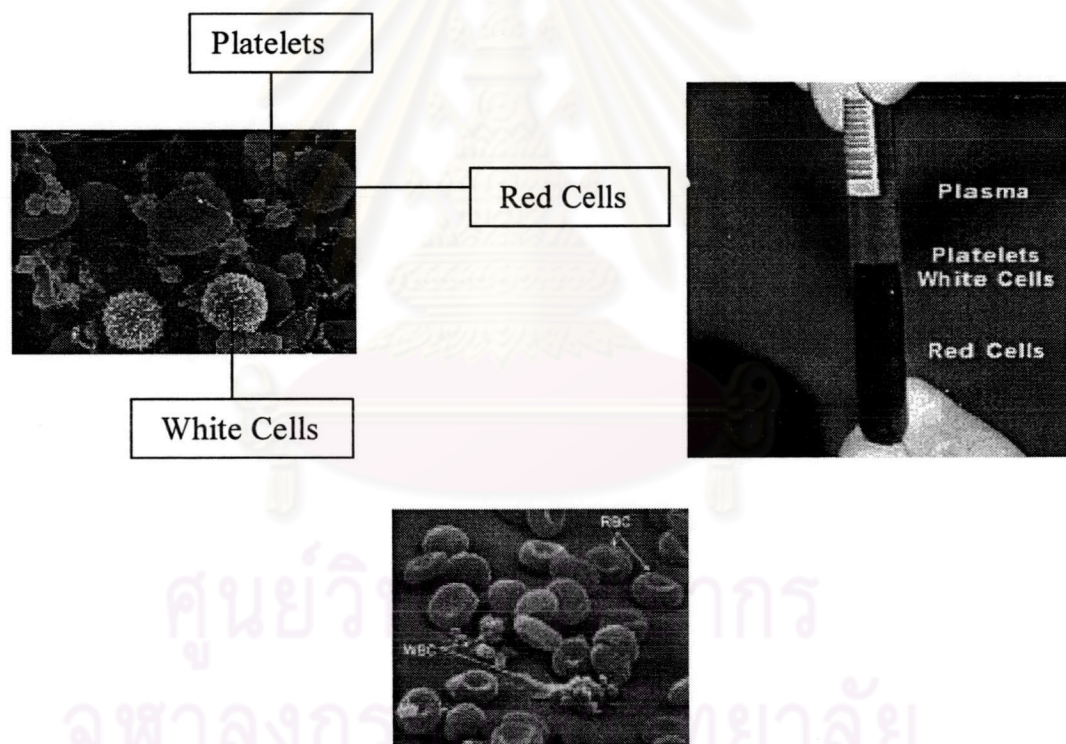


Figure 2.7 Pictorial representation of human blood [22].

Many specific functions of blood are carried out by proteins found in plasma. Human plasma contains a number of proteins such as albumin (Alb), immunoglobulins (Ig), complement factors, fibrinogen (Fg), Fibronectin (FN), coagulation factors (activators and down regulators), and lipoprotein (LP). These proteins all have various biological role: Alb is considered a biological passivator; immunoglobulin G (IgG) activates the complement system and, for example, binds

lymphocytes; the complement factors (including C3) are a part of immune defense ending in the lysis of cells with the membrane attack complex rupturing the cell types and bacteria have receptors for FN, α_2 -macroglobulin (α_2 M) is a down regulator of the coagulation cascade that ends in the formation of blood clot in which factors like high molecular weight kininogen (HMWK), factor XII (F XII), factor VII (F VII) and prekallikrein (PK) are component, anti thrombin III (A_{Th} III) is another potent down regulator of coagulation, as it binds thrombin, LP can act as transport protein of such agents as cholesterol [22].

2.5.2 Mechanism of Thrombus Formation on Polymer Surface

When artificial materials contact a living organism, severe biological responses are induced. Particularly, thrombus is formed when blood encounters a foreign surface as shown in Figure 2.8. The mechanism of coagulation is very complicated, but for simplicity can be classified into three processes: (1) the coagulation system, (2) the platelet system, and (3) the complemental system. The coagulation system can be further classified into two processes. One is started by Factor VII when the tissue is damaged extrinsically (i.e. outside the body). The other is induced by Factor XII (Hageman Factor) which is activated via an inflammation originating within the body (i.e. intrinsic pathway).

It is well known that platelets also contribute to thrombus formation. A foreign substrate induces adhesion and activation of platelets with the adsorbed protein layer serving as a controlling factor of the platelet response. The adhesion of platelets to a biomaterial surface is followed by the platelet release reaction taking place in the adhering platelets and then platelet aggregation on the surface.

The complement system can also be classified into two processes: (1) the classical pathway and (2) the alternative pathway. The classical pathway is started from the interaction between the immunocomplex contained within immunoglobulin G (IgG) or immunoglobulin M (IgM) and C1q in the C1 complex. The alternative pathway is started with C3a work for adhesion of leukocyte and activation of C5.

Table 2.5 Coagulation Factors [23].

Coagulation Factors		
Factor	Name	Plasma half-life (h)
I	Fibrinogen	72-96
II	Prothrombin	60
III	Tissue Factor or thromboplastin	--
IV	Ca ²⁺	--
V	Proaccelerin	15
VII	Proconvertin	5
VIII	Antihemophilic A factor	10
IX	Antihemophilic B factor or Christmas factor	25
X	Stuart factor	40
XI	Plasma thromboplastin antecedent	45-65
XII	Hageman factor	60
XIII	Fibrin Stabilising Factor	150
	Prekallikrein	--
	High-Molecular Weight Kininogen	156

These three mechanisms of coagulation are not independent. Normally, thrombus formation on a foreign surface results in an interaction between platelets and intrinsic pathway. Initiation of the intrinsic coagulation cascade may be induced by thromboplastins liberated from platelets or by Factor XII activation caused by platelets stimulated by released adenosine diphosphate (ADP). Thrombin formation caused by activation of the intrinsic pathway induces the production of a fibrin monolayer on a biomaterial surface and the promotion of platelet adhesion and aggregation.

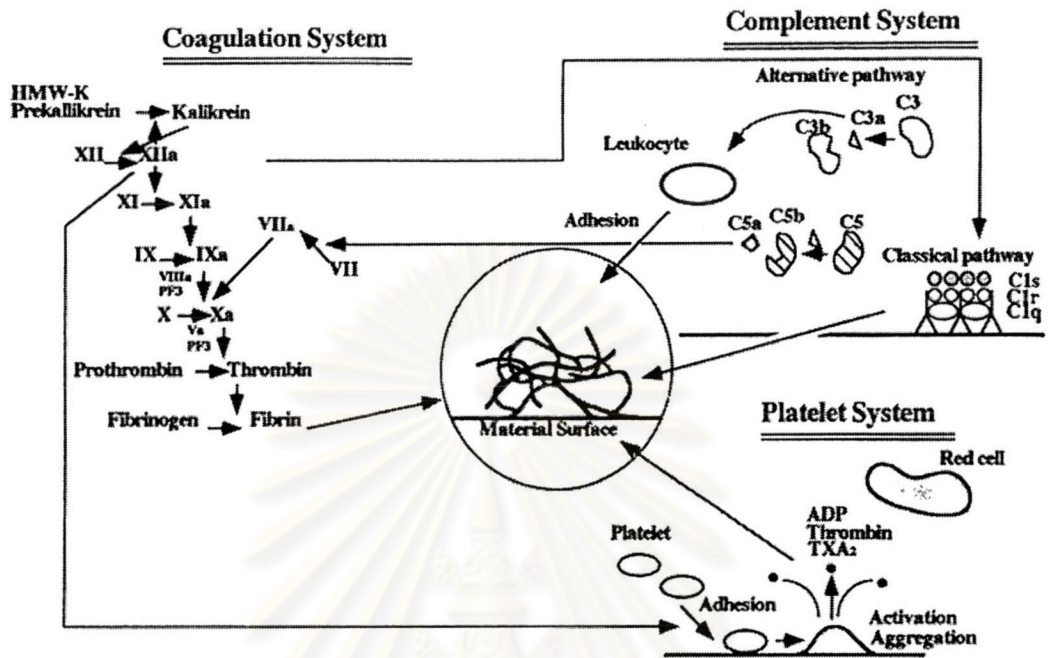


Figure 2.8 Schematic representation of blood coagulation system [23].

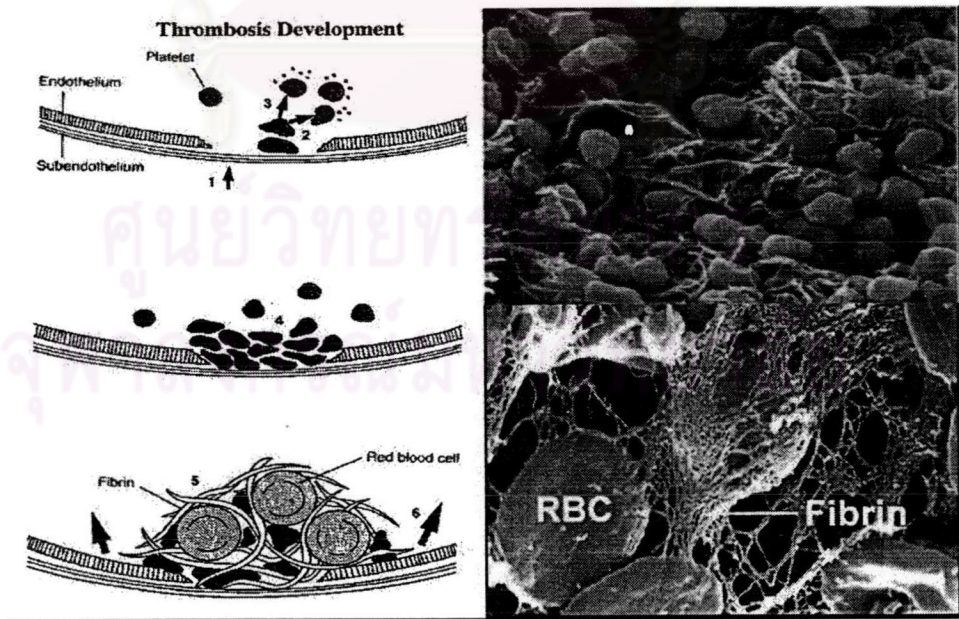


Figure 2.9 Schematic representation of fibrin formation in blood coagulation process [23].

2.6 Development of Blood-Compatible Polymer Surface

Biocompatibility is defined as the ability of a material to interface with a natural substance without provoking a biological response. In the human body the typical response to contact with a synthetic material is the deposition of proteins and cells from body fluids on the surface of the material. The human body tolerates plastics such as PVC, polycarbonate, polyurethane and the like for a short period of time, but the materials are not considered biocompatible for long-term usage.

Biopolymers as well as biomimetic and bioinert polymer structures are key components to create interfacial layers on established bulk materials. The application of *Biosurface Engineering* is facilitated by several powerful methods of surface functionalization including;

- Low-pressure-plasma-assisted surface modification
- Immobilization of bioactive molecules
- Polymer templates/ tissue engineering
- Plasma treatments
- Grafting of reactive chains
- Coating of functional layers

It was suggested that thrombogenicity could be decreased by polymer coating. Surface design aimed at reduced adhesion and preserved functions of platelet is of great importance for extracorporeal devices. A drastically reduced number of adhering platelets and significantly decreased simulation was achieved by coating technique using hydrophilic monomer. Examples of hydrophilic monomer are poly(methoxy-capped poly (ethylene glycol) methacrylate), poly(ethylene oxide) (PEO), poly(dimethyl acrylamide). Among the hydrophilic polymer, PEO and its derivatives are the most well known for this purpose [24, 25].

Nagaoka and Mori proposed the use of hydrated surface dynamic to improve blood compatibility by grafting poly(ethylene oxide) onto poly(vinyl chloride). They

demonstrated the excluded volume effect and the dynamic motion of the water soluble PEO chains on the surface suppressed protein adsorption and platelet adhesion. The movement of hydrated PEO chains induced the microflow of water, and the surface adsorption is inhibited. The effect of surface mobility of PEO chain and chain length are shown in Figure 2.10. For an irreversible adhesion, protein should be in contact with a foreign surface more than certain of time. PEO shows high mobility and hydration in water. Rapidly moving hydrated PEO chains on a surface will effectively prevent stagnation of the proteins on the surface, probably because the contact time is shortened. The mobility of the hydrated PEO chains increases with their chain length up to about 100, hence the long PEO chains are supposed to suppress the adsorption of proteins more effectively than shorter chains. PEO surfaces in water with rapidly moving hydrated PEO chains and a large excluded volume tend to repel protein molecules which approach the surface. The repulsive forces by the adsorbed PEO chain are generated by the loss of possible chain conformations, as the volume available to the adsorbed chains is reduced between approaching surfaces. PEO shows a large excluded volume in water and thus is very effective for steric repulsion as shown in Figure 2.10 [25].

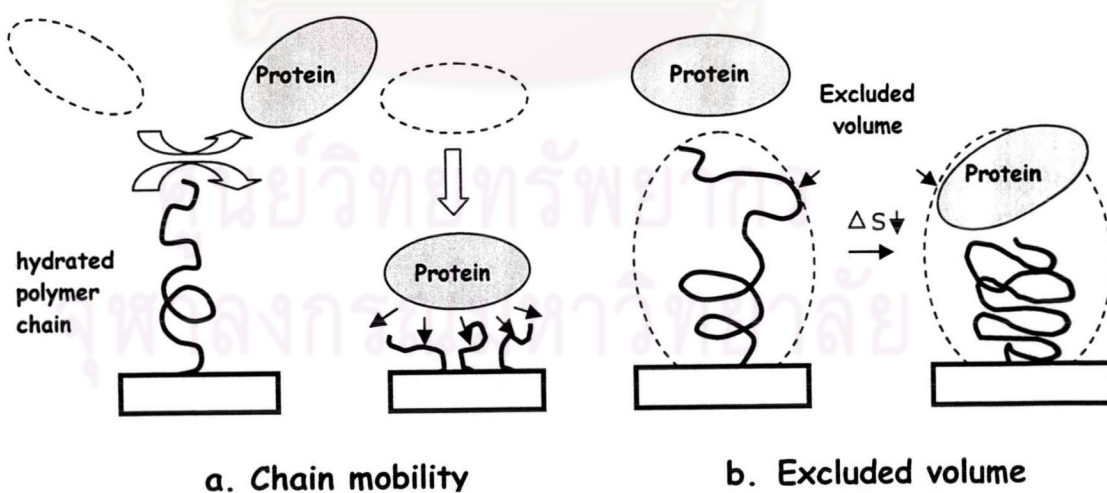


Figure 2.10 Chain mobility and excluded volume of PEO [24].

Recently, many research publications have reported the use of the grafting of hydrophilic monomer to modify and to improve the blood compatibility of the polymer surface for biomedical applications.

In 1997 Kuroda and coworkers prepared the surface grafting of α -propylsulfate-poly (ethylene oxide) (PEO-SO₃) on polyurethane surface and used *p*-azidophenyl as a photoinitiator. They used the heterodifunctional PEO derivative with sulfonate group at one end and a *p*-azidophenyl group at the other. The chemical structure of PEO-SO₃ and synthesis of *p*-azidophenyl derivatize α -propylsulfate sodium salt-poly (ethylene oxide) (MW 1000) and the grafting procedure are shown in Figure 2.11.

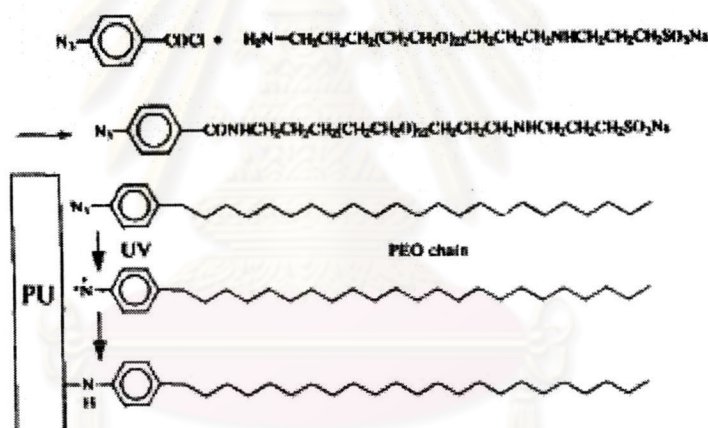


Figure 2.11 Synthesis of *p*-azidophenyl-derivatize α -propylsulfate sodium salt-poly (ethylene oxide) and photo-induced grafting technique using a *p*-azidophenyl group on a polyurethane surface.

The surface of polyurethanes (PUs) after modification showed anti-Factor Xa activity in the presence of antithrombin III factor (ATIII). The percentage of the platelet coverage of modified PUs was significantly decreased when compared with the unmodified PUs. They suggested that the decrease of platelet may be interpreted as 2 points. Firstly, the high hydrophilicity and high mobility of PEO graft chains may prevent adsorption of proteins. Secondly, negatively charged sulfonate groups may induce an electrical repulsion between the surface and platelet, which has negative surface charge derived from the sialic acid of cellular membrane

glycoproteins. From these results, they concluded that the grafting of PEO-SO₃ enhanced the antithrombogenicity of PUs surfaces [26].

In 1998, Nho and coworkers reported the blood compatibility of poly ethylene (PE) film grafted with poly(ethylene glycol) methacrylate (PEGMA). Different molecular weight of PEGMA (163-173, 261-283 and 387-468) was grafted onto PE film by a pre-irradiation grafting process. The extent of grafting was found to be dependent on the storage condition of the irradiated PE film, the pre-irradiated dose, reaction time and temperature, molecular weight of PEGMA and the type of solvent. The grafting yield was rapidly decreased with storage time for irradiated PE film stored at room temperature. On the other hand, the storage condition at -130°C, the grafting yield remained nearly constant up to 20 days after irradiation. The grafting yield was also decreased with increasing of PEGMA molecular weight. This may be due to the steric effect of the long polyether chain. As the ether chain increased in length, there is an increased probability that the vinyl group became shielded by the coil of the PEG group. The vinyl group may therefore be less accessible to radical attack. The water contact angle of grafted PE film decreased with the increasing of the grafting yield. The protein adsorption and platelet adhesion were significantly decreased with the increasing of grafting yield due to the hydrophilicity of the grafting layer [27].

In 2000, surface modification of emeraldine (EM) film by grafting of poly (ethylene glycol) methacrylate (PEGMA) (MW ~ 2,000) was reported by Kang and coworkers. The grafting yield of PEGMA onto EM film (PEGMA-g-EM) was increased as the UV graft copolymerization time and also PEGMA concentration increased. The contact angle decreased with the increasing grafting time. The surface morphology has been studied by AFM technique. After graft copolymerization the surface of EM became rougher. The protein adsorption and platelet adhesion were effectively reduced for the modified surface and increased with the increasing of grafting yield. The effectiveness in reducing protein adsorption and platelet adhesion was further enhanced through protonation of EM and PEGMA-modified EM films [28].

In 2002, Kang and coworkers studied the reduction of protein adsorption of poly(tetrafluoroethylene) (PTFE) film modified by plasma-induced graft polymerization of poly (ethylene glycol) methacrylate (PEGMA) ($M_w \sim 1,000$). The process involved Argon plasma-induced graft polymerization of PEGMA onto the H_2 plasma-pretreated PTFE surface (pp-PEGMA-g-PTFE).

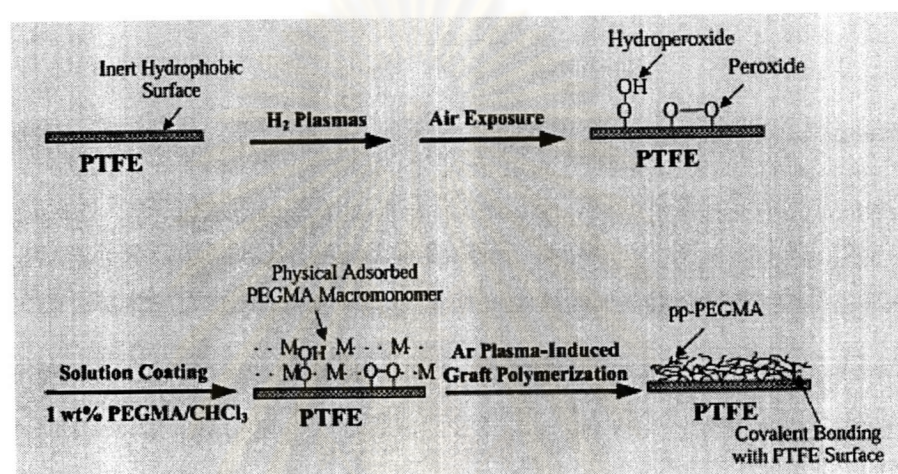
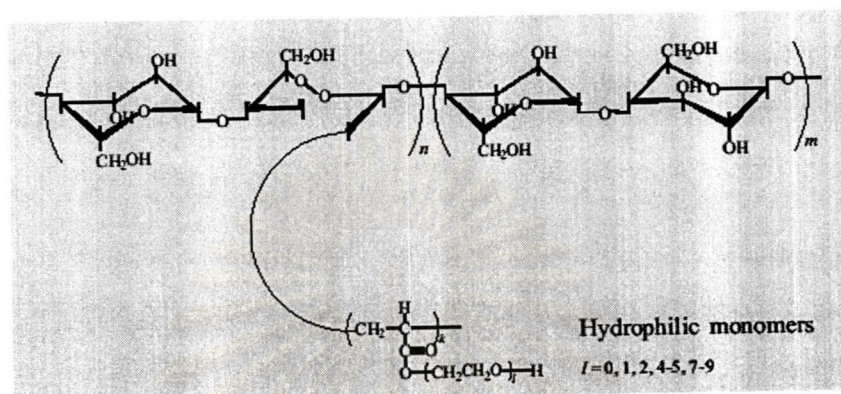


Figure 2.12 Schematic representation of the process of Ar plasma-induced graft polymerization of PEGMA on the H_2 plasma-pretreated PTFE surface.

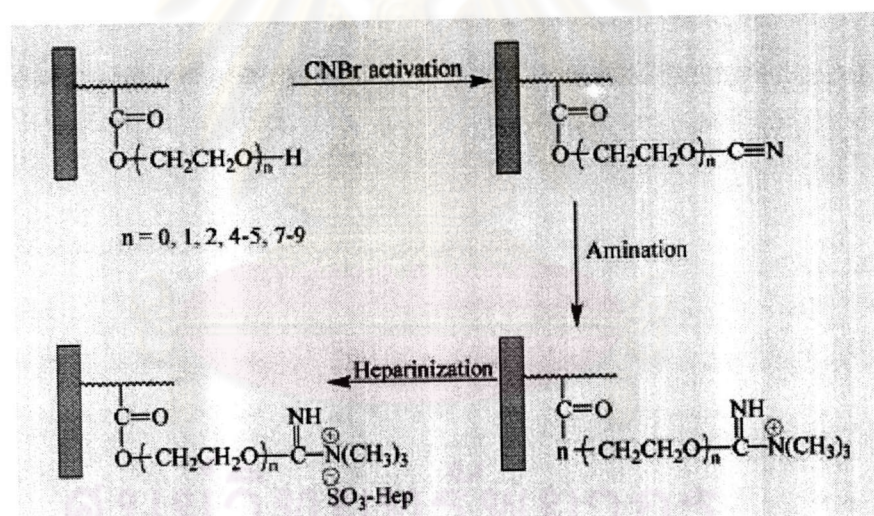
The graft concentration of the pp-PEGMA-g-PTFE increased with increasing RF power and glow discharge time of the Ar plasma. The PEGMA graft concentration was determined from the intensity peak XPS-derived $[C-O]/[C]$ ratio. The graft concentration reached about 0.70 for the pp-PEGMA-g-PTFE surface prepared at RF power = 15 Watt, pressure = 100 Pa, gas flow rate = 20 sccm and 60 second. The confirmation of grafting by water contact angle, FTIR, XPS and AFM showed that the grafting was successful. And the protein adsorption indicated that the pp-PEGMA-g-PTFE films could exhibit non-fouling surface characteristics [29].

In 2003, Nho and coworkers reported the improvement of blood compatibility of cellulose film for hemodialysis, by grafting with acrylic acid (AAc), 2-hydroxyethyl methacrylate (HEMA) and three kinds of poly (ethylene glycol) methacrylate (PEGMA). The structure of grafted cellulose film is shown in Scheme 2.3. As illustrated in Scheme 2.4, CNBr was selected as the activation reagent because it can activate hydroxyl groups that are abundant on cellulose surface after

grafting. The activated surface was then subjected to amination followed by heparin immobilization via ionic bonding.



Scheme 2.3 The chemical structure of grafted cellulose films.



Scheme 2.4 Schematic diagram showing grafting and heparin immobilization.

The grafting and heparinization were confirmed by ATR-IR technique, and electron spectroscopy. The carbonyl stretching ($>C=O$) peaks at 1730 cm^{-1} increased with increasing grafting yields. The CN and C=O stretching after heparinization appeared at 2260 cm^{-1} and 1730 cm^{-1} , respectively. The grafting yield was increased with an increasing reaction time and monomer molecular weight. The grafting yield was also affected by grafting temperature because the reactive sites on the cellulose substrate can be easily generated by the hydroperoxide dissociation at high temperature. The blood compatibility of modified cellulose was greatly improved.

As investigated by ESCA, the nitrogen peak from the peptide bond (O=C-N-) was used as an indicator of surface protein adsorption. The amount of protein adsorbed on modified surface was significantly decreased. The thrombus formation on grafted and heparinized-cellulose film surfaces was reduced. The considerable reduction of platelet adhesion on heparinized-cellulose film surfaces was also observed [30].

In the late '70s, Professor Dennis Chapman identified the phospholipids phosphorylcholine as an essential part of the cell membrane of red blood cells. He found that PC is a key factor for the resistance of the cell membrane against protein adsorption. Surface protein adsorption happens in a very short time (a few minutes) and is triggered by chemical and physical phenomena found in the surface composition of materials. Up to now, a large number of phospholipids have been identified in the human body. They are characterized by a similar molecular configuration, i.e. they consist of a hydrophobic tail and a hydrophilic head group. The biocompatible properties of phospholipids are believed to be based on this polarity configuration.

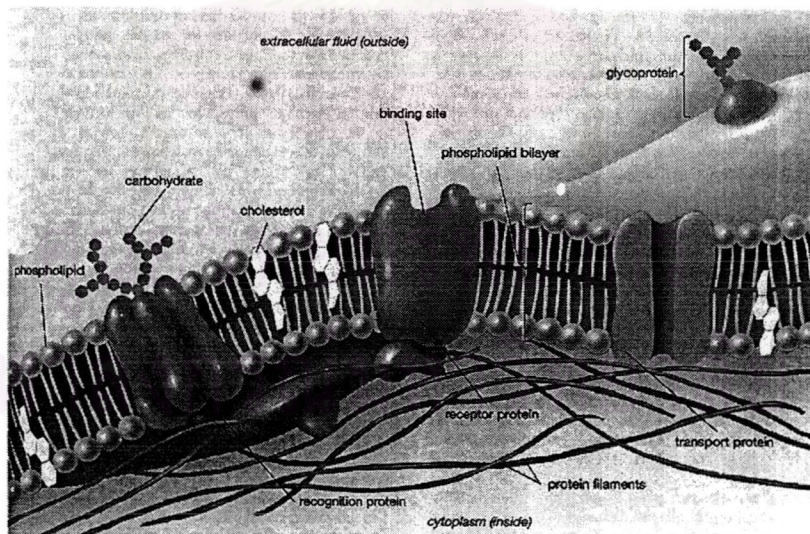


Figure 2.13 Structure of cell membrane [23].

The polymer that constitutes the phosphorylcholine coating is not soluble in water, but it assumes a hydration state when it is wet, with free water molecules that are not superficially bonded. Usually water molecules indeed tie to the hydrophobic part of a polymer by the van der Waals forces through a hydrophobic interaction mechanism. This water molecules' bonding mechanism generates then the phenomenon of protein adsorption, but when a protein molecule is adsorbed on a material surface there is an exchange of water molecules: the superficially adsorbed protein loses its solvation water in the part in contact, inducing a phenomenon of conformational change as the hydrophobic part of protein is exposed towards the material surface.

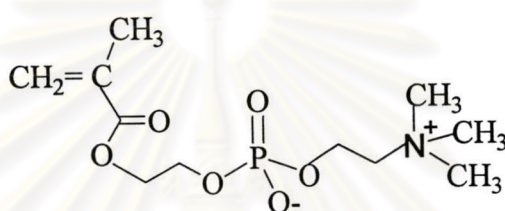
If the state of a water molecule on the surface of a material is similar to the one of an aqueous solution, then the proteins do not need to release their solvation molecules during contact with the surface and therefore hydrophobic interaction and conformational change will be suppressed.

The high presence of free water molecules on foreign surfaces treated with phosphorylcholine coating allow a reversible surface contact of protein molecules, and therefore avoids the conformational change and favours a higher grade of hemocompatibility of treated materials.

The coating of material surfaces with phosphorylcholine is an approach to modify the surfaces in such a way that they become biocompatible. Further researches lead to the development of a synthetic phosphorylcholine molecule which can be used to provide a uniform and continuous covering of various surfaces [29].

In 2000, Ishihara and coworkers reported the photo-induced graft polymerization of acrylamide (AAm), *N*-vinyl pyrrolidone (VPy), monomethacryloyl poly(ethylene glycol), 2-methacryloxyethyl phosphorylcholine (MPC) onto polyethylene (PE) film using 0.1 % W/V benzophenone as a photosensitizer. As analyzed by water contact angle measurement, it was found that the hydrophilicity linearly increased with an increasing in the photo-irradiation time. Surface analysis by ATR/FT-IR technique observed the new absorption after grafted with MPC, at 969 cm^{-1} which corresponded to the phosphate group. The XPS spectra of carbonyl

group of modified PE films confirmed the success of grafting. The grafting of the water-soluble polymer was effective for reducing the protein adsorption; however, the effects depended upon the chemical structure of the grafted polymer. The platelet adhesion was suppressed on the PMPC-g-PE membrane and PVPy-g-PE membrane even when the contact time of PRP was 3 h. On PMPEG-g-PE membrane, the platelet was hardly observed after the 3 h. Anyway the PAAm-g-PE membrane was not effective for platelet resistance [32].



Scheme 2.5 Chemical structure of MPC [32].

In 2002, Ishihara and coworkers studied the application of MPC for the hemocompatible separation membrane. Cellulose acetate (CA) membrane was blended with MPC and *N*-butyl methacrylate copolymer (PMB30) in order to prepare hemocompatible filtration system. CA and CA/PMB30 blended membranes with an asymmetric and porous structure were prepared by phase inversion process. The structure of PMB30 and ultrafiltration apparatus wear, are shown in Figure 2.14.

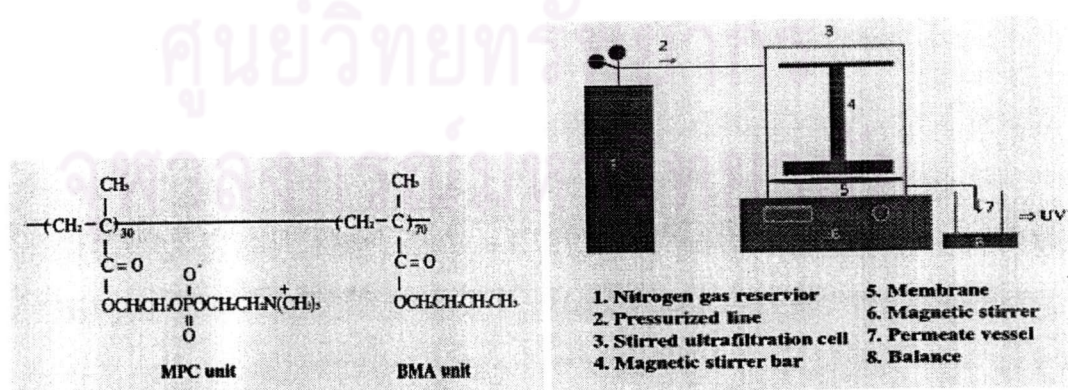
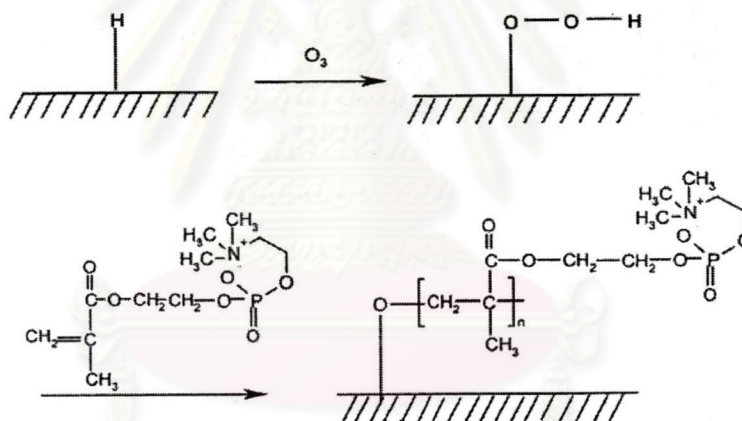


Figure 2.14 Structure of PMBA30 and schematic illustration of the ultrafiltration experimental apparatus.

The mechanical properties and solute permeability of the CA/PMB30 blended membrane could be controlled by preparation conditions such as the composition of the solvents and the solvent evaporation time. The CA/PMB30 blended membrane showed both good water and solute permeability. The molecular weight of the solute passing through the membrane was changed by the addition of PMB30. The CA/PMB30 blended membrane had the excellent blood compatibility due to the MPC unit in the PMB30 at the surface [33].

Recently, the grafting of phosphorylcholine polymer onto silicone film was reported by Lin and coworkers. MPC polymer was successfully grafted onto silicone film surfaces (PMPC-g-silicone) by ozonization as shown in Scheme 2.6.



Scheme 2.6 Illustration of surface graft copolymerization.

Graft copolymerization was confirmed by XPS and ATR-FTIR. The XPS results showed the content of N_{1s} [N⁺(CH₃)₃] and P_{2p} (PO₄) in the PMPC-g-silicone film. The ATR-FTIR spectra of PMPC-g-silicone showed the peaks of -POCH₂ at 1240 cm⁻¹ and 1080 cm⁻¹, >C=O at 1730 cm⁻¹ and [-N⁺(CH₃)₃] at 970 cm⁻¹. The hydrophilicity of PMPC-g-silicone was greatly enhanced and the grafted film's hydrophilicity increased with increasing MPC concentration. The platelet adhesion was absent on the grafted film even when the grafted film was immersed in PRP for 180 min. This result demonstrated that the antithrombogenicity of PMPC-g-silicone film was greatly improved [34].

The blood compatibility of natural rubber has been reported since 1989. Razzak and coworkers studied the radiation-induced grafting of *N, N*-dimethyl acrylamide (DMAA) and *N, N*-dimethylaminoethylacrylate (DMAEA) onto natural rubber tube. The grafting proceeded effectively in the presence of carbon tetrachloride (CCl_4) as a solvent. The grafting yield increased as a function of irradiation time and grafting temperature as well as monomer concentration. The clotting was still observed when the grafting yield was less than 30 wt%. The clotting disappeared when the grafting was higher than 30% [35, 36].

Later in 1992, Razzak and coworkers reported the blood compatibility of NR-g-DMAA assessed by three methods, *in vitro* test, *ex vivo* once through test and *ex vivo* loop test. The *in vitro* test, testing the blood clotting occurred as a function of grafting yield, 3.05, 15.45, 31.05 and 48.06 wt%, found that, the clotting decreased as a function of grafting yield. The higher grafting yield provided the better blood compatibility. The schematic of *ex vivo* once through test and *ex vivo* loops test are shown in Figures 2.15 and 2.16, respectively.

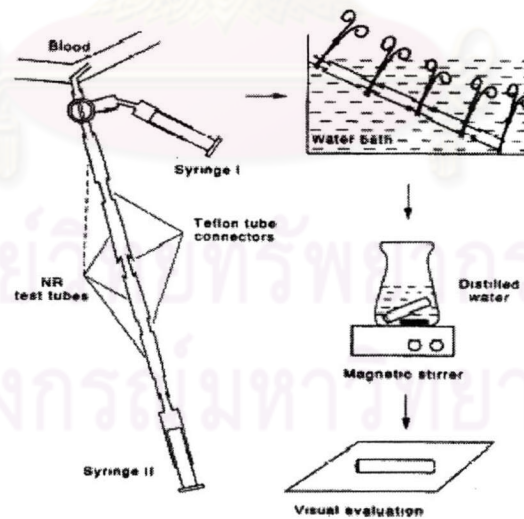


Figure 2.15 A device for *ex vivo* once through method and the experimental sequence.

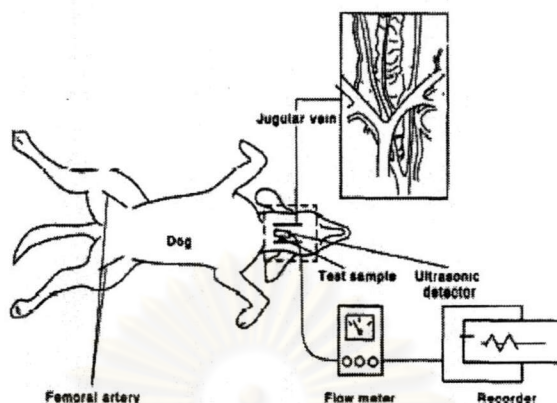


Figure 2.16 Schematic of ex vivo loops experimental showing jugular vein location of implanted sample and flow measuring and recording instrumentation.

The ex vivo loop test, was testing the circulation of blood flow, the NR-g-DMAA showed the better performance than the ungrafted NR tube and also the silicone rubber tube (SiR) even though the grafting yield of NR-g-DMAA was ~19 wt%. The blood flow through NR-g-DMAA tube continued smoothly for 60 min. Unlikely, The blood flow through ungrafted and SiR were almost stopped in 40 min. and 30 min respectively [37].

The most recent paper was reported by Kang and coworkers in 2001. They studied the surface modification of natural latex films with poly(ethylene glycol) methacrylate (PEGMA) by argon plasma followed by UV-induced graft copolymerization technique as shown in Figure 2.17.

The UV-induced graft copolymerization of PEGMA onto the plasma-pretreated NR latex rubber films was confirmed by contact angle measurement, atomic force microscopy (AFM) and XPS. The grafting yield depended on the grafting time and concentration of PEGMA. In general, higher monomer concentration and longer grafting time led to a higher grafting yield. The NR surface with a high density of grafted PEGMA was very effective in reducing protein adsorption and platelet adhesion. A lower grafting yield of the high-MW PEGMA was more effective than a high grafting yield of the low MW in reducing protein adsorption and platelet adhesion [38].

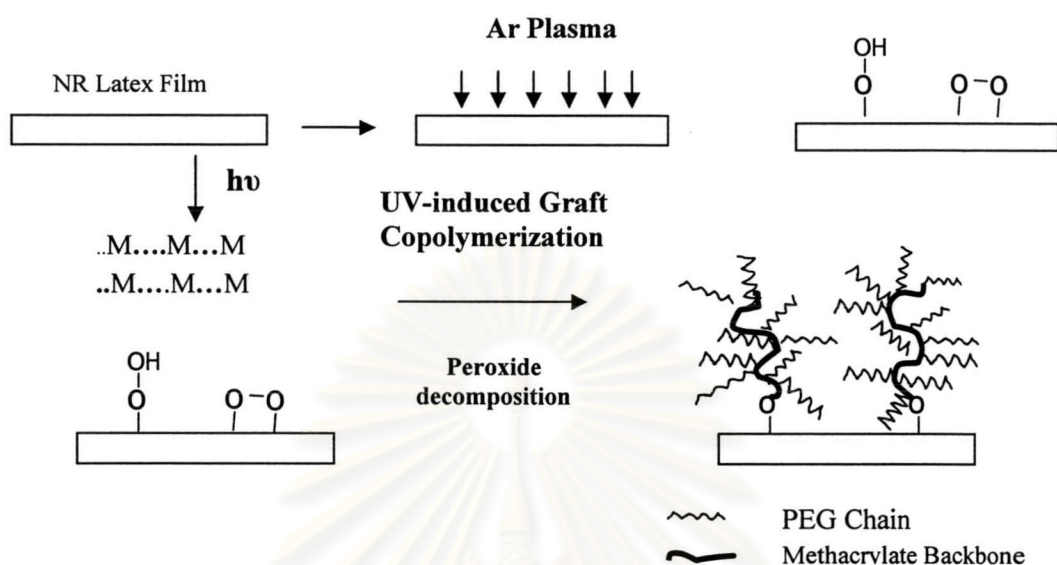


Figure 2.17 Argon plasma induced graft copolymerization.

2.7 Surface Characterization Techniques

Surface characterization is a method used for analyzing chemical and physical properties of material surface. In this research, surfaces were analyzed in order to confirm the success of graft copolymerization. The techniques that were used are as followed.

2.7.1 Attenuated Total Reflectance Infrared Spectroscopy (ATR-IR) [16, 39]

In attenuated total reflectance infrared spectroscopy (ATR-IR) a beam of infrared light is totally reflected inside a specially cut infrared transparent material which has a high index of reflection. The infrared beam from the spectrometer is focused onto the beveled edge of an internal reflection element (IRE). The beam is then reflected, generally numerous times, through the IRE crystal, and directed to a detector. Figure 2.18 shows the typical geometry employed for ATR experiments.

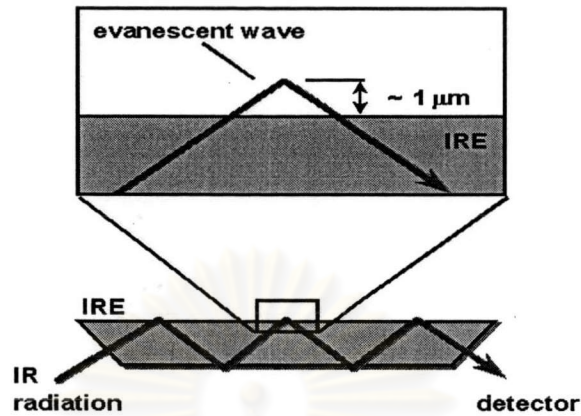


Figure 2.18 Diagram of ATR-IR [39].

Typical materials used for ATR prism are Ge, Si and ZnSe. Because the index of reflection differs from polymer and the prism, an evanescent wave penetrates the polymer if the two are in intimate contact. The infrared radiation will interact with molecule vibrations in the same manner as in conventional infrared spectroscopy. The amplitude of the evanescent wave decays exponentially from the surface and the depth of penetration is arbitrarily described as the point where the amplitude decays to 37 % of its initial value. The depth of penetration depends on the ratio of the reflective indexes between the polymer and the prism, the angle of incidence, and the frequency of radiation in the following equation:

$$d_p = \frac{\lambda}{2\pi n_p (\sin^2 \theta - n_{sp}^2)^{1/2}} \dots\dots\dots(3)$$

where λ = wavelength of the radiation in the IRE, θ = angle of incidence, n_{sp} = ratio of the refractive indices of the sample vs. IRE, and n_p = refractive index of the IRE. Practically, the sample is placed in close optical contact with one of the crystal. In this study, ATR-IR was used for identifying functional groups on the surface of modified rubber surface. Sampling depth of characterization is 1-1.5 μm .

2.7.2 Contact Angle Measurement [16, 40]

Contact angle is considered as one of the most surface-sensitive techniques and can provide information on outermost few angstroms of solids. The equipment required is relatively simple and inexpensive. The basis of the contact angle technique is the three-phase equilibrium at the contact point at the solid/liquid/vapor interface (Figure 2.19).

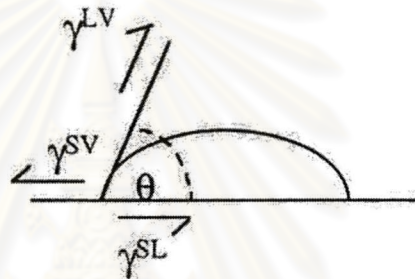


Figure 2.19 Contact angle geometry indicating the three-phase equilibrium [16].

It can be seen from Figure 2.20 that low values of θ indicate that the liquid spreads, or wets well, while high values indicate poor wetting. If the angle θ is less than 90° the liquid is said to wet the solid. If it is greater than 90° , it is said to be non-wetting. A zero contact angle represents complete wetting.

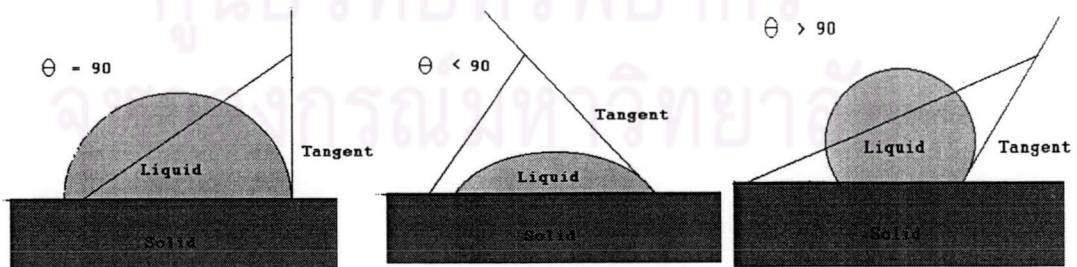


Figure 2.20 A liquid droplet in equilibrium with a horizontal surface surrounded by a gas. The wetting angle (θ) between the horizontal layer and the droplet interface defines the wettability of the liquid. To the left: A non-wetting fluid with $0 \leq \theta \leq 90^\circ$. To the right: A wetting fluid with $90^\circ \leq \theta \leq 180^\circ$ [40].

The contact angle was associated to the surface energy of the solid and the liquid surface tension by Young in 1850. The calculation is based on the energy balance approach to the three-phase equilibrium. The cosine contact angle ($\cos\theta$) is directly related to the surface energy by Young's equation, where γ^{sv} , γ^{sl} and γ^{lv} are the surface tension of the solid-vapor, solid-liquid, liquid-vapor interfaces, respectively.

$$\gamma^{sv} - \gamma^{sl} = \gamma^{lv} \cos\theta \quad \dots\dots\dots(4)$$

Direct interpretations from this equation can be made based on several assumptions that predict only one intrinsic contact angle (θ_0) regardless of how that angle is measured. The assumptions are:

1. The solid surface is rigid and non deformable (surface modulus > 3.5×10^5 dynes/cm²).
2. The solid surface is highly smooth.
3. The solid surface is chemically homogenous.
4. The solid surface does not interact in any way with the liquid other than the three-phase equilibrium (i.e. swelling).
5. The surface functional groups do not reorganize in response to change in the environment during the measurement.
6. The liquid must not cause extraction or partitioning of material from the solid phase to the liquid phase.

In practice, some of these assumptions are generally not valid and the observed contact angles depend on the way they are obtained. Generally, two contact angle values are measured (see Figure 2.21). The advancing contact angle (θ_A) can be measured as the solid/liquid contact area increases. The receding contact angle (θ_R) can be measured as the solid/liquid contact area decreases.

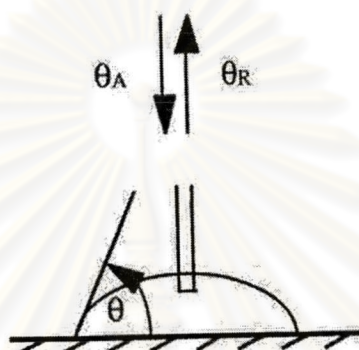


Figure 2.21 Measurement of advancing/receding contact angles (θ_A/θ_R) [16].

ศูนย์วิทยทรัพยากร
จุฬาลงกรณ์มหาวิทยาลัย